Analysis of Interface Evolution and Pattern Formation During CVD

Jacob J. Thiart and Vladimir Hlavacek
Laboratory for Ceramic and Reaction Engineering, Dept. of Chemical Engineering,
State University of New York at Buffalo, Amherst, NY 14260

Morphological aspects of the evolution of a gas–solid interface during typical CVD processes are presented, as well as a continuum model of CVD growth. A linear stability analysis used determines the effect of reactor conditions on the stability of planar growth. The main focus, however, is numerical solution of governing equations under a wide variety of conditions and with different initial interface shapes as starting point. Simplified solutions under specific deposition conditions and the numerical procedure for solving the complete system of equations are presented. The focuses are on the use of a parametrization that eliminates numerical problems encountered with steep interface gradients and the automatic generation of an adaptive mesh for the domain above the interface. Several examples illustrate the numerical solution procedure. To our knowledge, this is the first attempt to simulate interface evolution during CVD for long deposition times from various initial interface shapes. The simulation revealed several morphological phenomena observed experimentally in previous studies, including the formation of occlusions that contributes to film porosity and was clearly shown by the numerical results. Film uniformity strongly depends on the controlling mechanism of deposition. Severe nonuniformities develop under diffusional limitations, while deposition is very uniform under conditions of kinetics control. Film uniformity could be improved by choosing conditions for which a Damköhler number of deposition, Da, would have the lowest value.

Introduction

Requirements of purity, electrical and mechanical properties of films in electronic, structural, engineering and coating applications have become increasingly difficult to achieve. Film morphology during chemical vapor deposition (CVD) plays an important role in determining properties relevant in thin film applications. Experimental efforts to characterize and control film morphology have led to a classification of morphology in terms of zones of specific morphology as a function of reactor conditions (Movchan and Demchishin, 1969; Thornton, 1974). Although useful, this information does not identify underlying phenomena or explain their relative importance. Some attempts have been made at studying the problem of film morphology during vapor deposition more fundamentally. Under low-pressure deposition, the mean free path (MFP) in the gas is larger than typical substrate sizes, which means transport of reactant to the substrate takes place ballistically. Under these conditions, Monte Carlo simulations of discrete particles have proved very useful in predicting film morphology, and good agreement between experimental observations and simulation results were obtained (Tait et al., 1990). However, the method is computationally very expensive. Singh and Shaqfeh (1993) used a continuum approach and showed simulation results of deposition with surface reemission under different sticking coefficients (see also Cale and Raupp, 1990).

A continuum approach lends itself better to studying the underlying phenomena, and allows the analysis of film stability to arbitrary perturbations (Palmer and Gordon, 1988, 1989; Van den Brekel and Jansen, 1978a,b). Typically, the height of the gas–solid interface (say H) is expressed as a function of the horizontal coordinate (say x) and physical phenomena such as surface diffusion, which depend on interface shape,

Correspondence concerning this article should be addressed to V. Hlavacek.

are accounted for by terms containing the appropriate spatial derivatives. The resulting problem belongs to the class of free-boundary problems, which occur in many important scientific and technological processes. These include among others, two-phase flow through porous media, flow in a Hele–Shaw cell, flame propagation in combustion theory, catalyst deactivation by plugging, solidification processes, etching processes, and growth of bacteria (Pelce, 1988; Hoffmann and Sprekels, 1990).

In a previous study (Viljoen et al., 1994; Thiart et al., 1994) we presented a continuum model for evolution of the gas–solid interface during typical atmospheric pressure CVD processes. Concentration of reactant in the gas phase and the interface shape were solved in Cartesian coordinates by successive solution at each instant in time. It was assumed that the interface position could be expressed as a single-valued function of the horizontal coordinate, which is acceptable for deposition under many realistic process conditions. Satisfactory results were obtained for cases where deposition was not severely limited by gas-phase mass transport. However, there are real cases where expression of the interface as a single-valued function becomes inappropriate. Experimental results of Van den Brekel (1977) showed fingerlike growth under diffusion-limited growth conditions, which illustrate this point. Indeed, under these conditions the simulations could be continued only up to a point where interface gradients approached infinity, and therefore caused numerical difficulties.

This study proposes a solution procedure that can overcome the problems encountered with infinite gradients. We address the problem of highly irregular interface shapes during typical CVD processes, and present a parametrization that eliminates the numerical difficulties encountered before. The continuum model of gas–solid interface evolution is presented first, after which a linear stability analysis is performed. The focus then shifts to numerical solution of the governing equations. Special cases where the system of coupled equations can be simplified and solved more easily are highlighted. The numerical procedure for solution of typical CVD cases with highly irregular interface shapes is presented, with emphasis on an appropriate parametrization, as well as automatic adaptive mesh generation. Numerical examples are then used to illustrate application of the solution method and to identify parameters that have the most significant effect on film morphology during CVD.

Model of CVD Growth

Under low-pressure operation, with a ballistic transport and deposition mode, the flux of reactants to the interface can to a good approximation be represented as a known constant or as a function of the incident angle or local interface curvature (Bales and Zangwill, 1991; Mazor et al., 1988). The problem then simplifies to solving for the position of the interface only, for which appropriate numerical techniques are well known. However, under atmospheric pressure conditions, transport to the interface is diffusive, rather than ballistic. The MFP of the gas is very short compared to the typical length of surface features. Interface growth depends on the concentration field in the gas phase above it, which in turn depends on the shape of the interface. The resulting coupled nonlinear initial-boundary-value problem is similar to solidification problems, where the shape of the liquid–solid interface is unknown and depends on the temperature field in the surrounding liquid and solid.

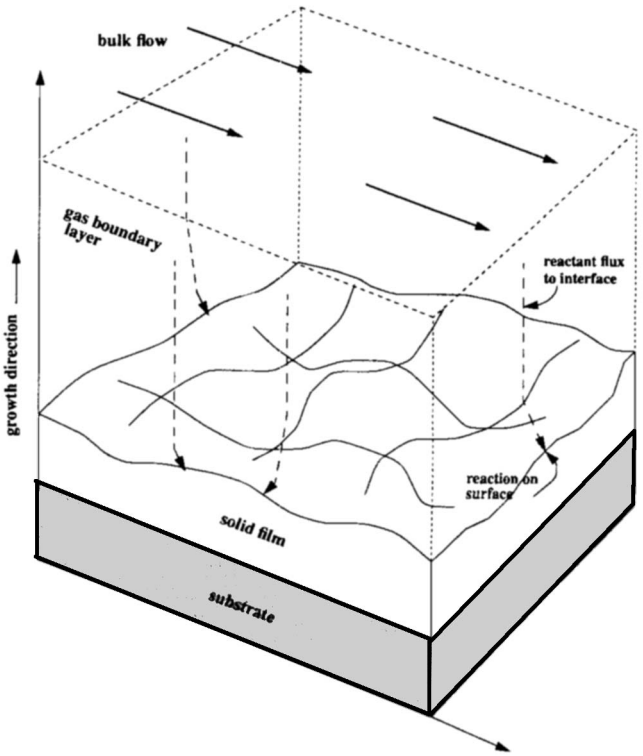

Figure 1. Modeling setup of growing film during CVD.

Consider the growth of an amorphous solid film during a typical high-pressure (0.1 to 1 atm) CVD process (Figure 1). The growth process consists of different subprocesses, including the following: (1) transport of reactants to the interface, (2) adsorption and desorption of reactants, (3) transport of adsorbed species along the interface, (4) surface reaction of adsorbed reactants to form solid product, (5) transport of solid material along the interface, and (6) transport of gaseous products away from the interface.

Although the physical problem is three-dimensional, we can simplify the analysis somewhat by considering changes in only one horizontal direction. Thus the gas-phase model will become 2-D and the gas–solid interface will be described in 1-D. This simplification is especially helpful when numerical simulations of interface evolution are proposed, since 3-D simulations can be computationally prohibitive. Let us consider the different subprocesses in more detail.

Gas phase

The mode of reactant transport to the film interface is assumed to be diffusion through a boundary layer. The thickness of this layer, δ, is typically much larger than the characteristic length of surface features, which means we can assume the top boundary of this layer to be flat (for slab geometry) and therefore unaffected by surface protrusions. The reactant concentration (C_b) in the bulk flow is assumed to be constant and not dependent on axial position in the reactor.

At the interface the adsorption, desorption, and surface reaction can be presented as

$$A + \bigstar \overset{k_{ad}, k_{des}}{\rightleftharpoons} A\bigstar \tag{1}$$

$$A\bigstar \overset{k_1}{\rightarrow} P, \tag{2}$$

where A is the gaseous reactant, $\bigstar$ represents a surface site, and P is the solid product. Note that the surface reaction is assumed to be irreversible. A conservation balance of the surface intermediate $A\bigstar$ takes the form:

$$\frac{dC_{A\bigstar}}{dt} + D_{fs}\nabla_s^2 C_{A\bigstar} = k_{ad}C_A(C_t - C_{A\bigstar}) - k_{des}C_{A\bigstar} - k_1 C_{A\bigstar}, \tag{3}$$

where the second term on the lefthand side represents the transport of adsorbed species along the surface and C_t is a constant denoting the concentration of all sites, vacant and occupied. Typically, under conditions of epitaxial growth the temperature is high and film growth very slow, so that the surface mobility of adsorbed species is relatively high. However, we are interested in growth of amorphous films, where surface mobility is relatively low and growth rates fast. This means that the surface mobility term in Eq. 3 can be neglected for cases we consider. This term should not be confused with the surface diffusion of solid species which is driven by interface curvature. The latter effect will be discussed in the next section. If we make the steady-state approximation for $C_{A\bigstar}$ and assume that the rate of surface reaction is much slower than that of adsorption/desorption ($k_1 \ll k_{ad}$, k_{des}), one finds the well-known expression

$$\Phi_A = \frac{K_{AD}C_A}{K_{AD}C_A + 1}$$

where $\Phi_A = C_{A\bigstar}/C_t$ is the fractional coverage. Let us furthermore assume that $K_{ad}C_A \ll 1$, which leads to

$$\Phi_A = K_{AD}C_A. \tag{4}$$

At this point we have not included the effect of an irregular surface on the adsorbed concentration. Thus, Eq. 4 represents the fractional coverage on a flat interface during growth of an amorphous film. In the presence of protrusions, the effect of capillarity tends to minimize surface energy and the result is that less reactant will be adsorbed on protrusions than in depressions. This effect is expressed by the Gibbs-Thompson relation (Mullins, 1957):

$$\Phi_A = K_{AD}C_A(1 + \Gamma\kappa)$$

where κ is the local curvature defined as negative for convex parts and positive for concave parts (viewed from the gas phase) and Γ is the capillary length defined as

$$\Gamma = \frac{\gamma\Omega}{K_B T}.$$

The surface reaction is assumed to be first order with respect to adsorbed reactant, thus the reaction rate is given by

$$R(C_A) = kK_{AD}C_A(1 + \Gamma\kappa) \tag{5}$$

where $k = k_1 C_t$. At the interface the reaction of adsorbed species is balanced by the flux of reactant to the surface. The length of the substrate is much larger than the typical size of surface features, and boundary conditions in the horizontal direction are therefore taken as periodic. Now introduce the following nondimensional variables:

$$\xi = \frac{x}{L}, \quad \zeta = \frac{z}{L}, \quad \mathfrak{C} = \frac{C}{C_b}, \quad \tau = \frac{tV_0}{L},$$

where V_0 is a reference growth rate and L is a characteristic length scale. It seems most convenient to choose this scale as the capillary length, thus $L = \Gamma$. The gas phase becomes (dropping the subscript for A)

$$\frac{\partial \mathfrak{C}}{\partial \tau} = \frac{1}{Pe}(\nabla^2 \mathfrak{C}) \tag{6}$$

with boundary conditions

$$\mathfrak{C} = 1 \quad \text{at} \quad \zeta = \frac{1}{\eta} + \frac{V}{V_0}\tau,$$

$$(\nabla \mathfrak{C} \cdot \boldsymbol{n}) = \eta Da\, \mathfrak{C}(1 + \kappa) \quad \text{at} \quad \zeta = \mathfrak{K},$$

$$\left.\frac{\partial \mathfrak{C}}{\partial \xi}\right|_{\xi = 0} = \left.\frac{\partial \mathfrak{C}}{\partial \xi}\right|_{\xi = nl/\Gamma},$$

$$\mathfrak{C}(0, \zeta) = \mathfrak{C}\left(\frac{nl}{\Gamma}, \zeta\right) \quad \text{with} \quad n = 0, \pm 1, \pm 2, \ldots, \tag{7}$$

and where $\mathfrak{K}$ represents the position of the interface and κ the dimensionless curvature. The dimensionless parameters are defined as

$$Pe = \frac{V_0 L}{D_f}, \quad Da = \frac{K\delta}{D_f}, \quad \eta = \frac{\Gamma}{\delta},$$

where $K = kK_{AD}$.

Solid phase

Growth in the solid phase is equivalent to the interface moving at a rate v normal to its previous position. This rate is determined by two factors, namely, growth as a result of surface reactions and flattening of protrusions by surface diffusion of solid species. Thus

$$v = \frac{\beta C_b \eta Da}{Pe}\mathfrak{C}(1 + \kappa) - \frac{\phi}{Pe}\frac{\partial^2 \kappa}{\partial s^2} \tag{8}$$

where

$$\phi = \frac{D_s^*}{D_f \Gamma} \quad \text{and} \quad D_s^* = D_s \Omega \alpha$$

and α is the number of molecules per unit surface area, and D_s the surface diffusivity. The last term represents the effect of surface diffusion (Mullins, 1957) with s the arc-length along the interface. The parameter $\Omega\alpha$ gives an indication of the thickness of solid film that participates in the surface diffusion phenomenon. If it is very small, only a thin top layer of solid has sufficient mobility to be affected by the surface diffusion process, and the solid beneath it is considered immobile. For modeling purposes this parameter is grouped with D_s to form a modified surface diffusivity D_s^* with units m^3/s. It is assumed to have an exponential temperature dependence. The parameter ϕ therefore represents a dimensionless form of effective surface diffusivity.

The deposition rate V represents the vertical component of interface growth. If we take the planar growth rate as a reference and assume that the vertical component of growth during nonplanar conditions is roughly the same as during planar growth, the top position of the gas boundary layer is given by $\zeta = 1/\eta + \tau$.

The Peclet number, Pe, gives an indication of the relative magnitude of convection and diffusion effects. In this problem, convection refers to the effect of interface movement, and the value of Pe is extremely small for most cases since film growth is so slow relative to gas diffusion. The Damköhler number, Da, gives an indication of the relative magnitude of gas diffusional and surface kinetic resistance, or alternatively, the relative rate of surface kinetics and gas diffusion. Several different forms of the Damköhler number have been used (Carberry, 1976; Levenspiel, 1972) for identifying whether mass-transfer limitations are present, or not. Typically a process is kinetically controlled for small values of Da, in which case the rate of diffusion is relatively fast ($Da \ll 1$). As the value of Da increases, surface kinetics become faster and thus comparable to the rate of diffusion. This represents a transition regime ($Da \approx 1$). For large values of Da, surface kinetics become extremely fast and the process becomes severely mass-transfer limited ($Da \gg 1$). The Damköhler number has a strong effect on the morphology of CVD growth, as will be illustrated later with numerical examples.

In general, one also has to formulate energy balance equations for both the gas and solid phases, which would enable you to determine the temperature along the interface and in the gas boundary layer. These equations would be coupled to the concentration balance and interface evolution equations, which greatly complicates the problem. In addition, physical properties such as the gas diffusivity (D_f), surface diffusivity (D_e), and capillary length (Γ), as well as the rate constant (K) also depend on temperature. The temperature distribution will strongly depend on reactor configuration. In a *cold-wall* reactor the substrate is heated directly (resistively) and maintained at a higher temperature than the outer walls. In this case, severe temperature gradients can be present, and Ananth and Gill (1992) showed that a negative gradient through the solid film can stabilize planar film growth. In a *hot-wall* reactor external heating of the substrate is achieved through radiation, and thermal gradients are typically much less severe than in the *cold-wall* configuration. To make the problem more tractable, we will assume the *hot-wall* configuration. The temperature of the solid film is assumed constant and the gas boundary layer is in thermal equilibrium with the solid. Temperature dependence of physical properties and parameters will be taken into account, but temperature now acts as a parameter, which can be chosen arbitrarily.

Table 1. Range of Parameters for Typical CVD Process

Parameter	Typical Value	Parameter	Typical Value
T (K)	900–2,000	D_s^* (m^3/s)	10^{-22}–10^{-17}
P (atm)	0.1–1.0	E_{a-s} (kcal/mol)	20–150
% dilution	90–99	E_{a-r} (kcal/mol)	20–80
δ (m)	10^{-4}–10^{-3}	K_0 (m/s)	10^{4}–10^{8}
D_f (m^2/s)	10^{-6}–10^{-4}	Γ (m)	10^{-12}–10^{-10}

For the cases considered in this article, we choose parameters in the range typical for the CVD growth of, for example, SiC and CrB_2, thus temperatures higher than 900 K and atmospheric pressure. Some properties, such as surface diffusivity and surface tension are not well-known for all solid materials. Nevertheless, we can define a range of typical values for deposition conditions, physical properties, and parameters, as shown in Table 1 (based on values in Kingery et al., 1976; Kristyan and Olson, 1991; Mazor et al., 1988; Van den Brekel, 1977; Mullins, 1957, 1959; Palmer and Gordon, 1989). The functional form of the temperature dependence of K, D_f, D_s^* and Γ is shown in Table 2.

Planar Solution

The system of equations has an analytical solution if the interface remains planar. Under these conditions the reactant concentration in the boundary layer is given by

$$\mathcal{C}_0(\zeta) = \frac{1}{\beta C_b}\left[\left(\frac{Pe + \eta Da}{\eta Da}\right) - \exp(-Pe\zeta)\right]. \tag{9}$$

The corresponding solid phase equation becomes

$$\left(\frac{Pe + \eta Da}{\eta Da}\right) - \exp[-Pe\delta/\Gamma] - \beta C_b = 0, \tag{10}$$

from which we can determine the growth rate V_0 (since Pe depends on V_0) for different operating conditions. The reactant concentration at the interface is given by

$$\mathcal{C}_0(0) = \frac{Pe}{\beta C_b \eta Da}. \tag{11}$$

This expression illustrates the effect of the Damköhler number, Da, on reactant concentration at the interface. An increase in the value of Da represents an increase in diffusional resistance, which leads to a decrease in $\mathcal{C}_0(0)$.

Table 2. Functional Form of Temperature-Dependent Parameters

Parameter	Functional Form	Reference
K	$K_1\exp[-K_2/T]$	Froment and Bischoff (1990)
D_f	$K_3 T^{K_4}$	Bird et al. (1960)
D_s^*	$K_5\exp[-K_6/T]$	Srolovitz et al. (1988)
Γ	K_7/T	Van den Brekel and Jansen (1978a,b)

Stability of Planar Interface

Although planar growth is usually preferred it is not easily achieved in practice. Anisotropic effects and impurities can create irregularities and protrusions on the surface. Preferential growth of these protrusions will take place due to higher reactant concentrations at their tips than at their bases. On the other hand, surface diffusion and capillarity tends to smooth any irregularities and has a stabilizing effect on planar growth. The relative magnitude of these effects will determine whether the growing interface is inherently stable, or not. In this section we will study the role of stabilizing and destabilizing effects on planar film growth. A linear stability analysis (LSA) often yields valuable information about appropriate deposition conditions for ensuring uniform films. A small sinusoidal perturbation is imparted to the basic solution (in our case planar interface) and it is determined whether the perturbation will grow or decay under specific deposition conditions.

Since only small deviations from planar conditions will be considered, we can express the growth equation in terms of the vertical translation of the interface ($\partial H/\partial\tau$) and transform to coordinates moving with the interface (Viljoen et al., 1994). The revised gas and solid phase equations become

$$\frac{\partial \mathcal{C}}{\partial \tau} = \frac{1}{Pe}\nabla^2 \mathcal{C} + \frac{\partial \mathcal{C}}{\partial \zeta} \tag{12}$$

with boundary conditions

$$\mathcal{C} = 1 \quad \text{at} \quad \zeta = \frac{1}{\eta},$$

$$(\nabla \mathcal{C} \cdot \boldsymbol{n}) = \eta Da\, \mathcal{C}(1+\kappa) \quad \text{at} \quad \zeta = \mathcal{H},$$

$$\left.\frac{\partial \mathcal{C}}{\partial \xi}\right|_{\xi=0} = \left.\frac{\partial \mathcal{C}}{\partial \xi}\right|_{\xi = nl/\Gamma},$$

$$\mathcal{C}(0,\zeta) = \mathcal{C}\left(\frac{nl}{\Gamma}, \zeta\right) \quad \text{with} \quad n = 0, \pm 1, \pm 2, \ldots \tag{13}$$

and for the solid phase

$$\frac{\partial H}{\partial \tau} = \frac{\beta C_b}{Pe}(\nabla \mathcal{C} \cdot \boldsymbol{n})\sqrt{1+H_\xi^2} - 1 - \frac{\phi}{Pe}\left[\frac{\kappa_\xi}{\sqrt{1+H_\xi^2}}\right]_\xi \tag{14}$$

with boundary conditions

$$H(0) = H(nl/\Gamma),$$

$$H_\xi(0) = H_\xi(nl/\Gamma),$$

$$H_{\xi\xi}(0) = H_{\xi\xi}(nl/\Gamma),$$

$$H_{\xi\xi\xi}(0) = H_{\xi\xi\xi}(nl/\Gamma), \text{with } n = 0, \pm 1, \pm 2, \ldots \tag{15}$$

and where

$$\kappa = -\frac{H_{\xi\xi}}{\left(1+H_\xi^2\right)^{3/2}}.$$

An interesting point to note is that the surface diffusion term contains a highly nonlinear fourth-order spatial derivative, which is unusual, since diffusion terms are normally of second order.

For the LSA, perturb the concentration and height of the interface as follows:

$$\mathcal{C}(\xi,\zeta,\tau) = \mathcal{C}_0(\zeta) + \epsilon \mathcal{C}_1(\xi,\zeta,\tau) + \ldots$$

$$H(\xi,\tau) = H_0 + \epsilon H_1(\xi,\tau) + \ldots$$

where trial functions of the form

$$\mathcal{C}_1(\xi,\zeta,\tau) = \mathcal{C}^*(\zeta) e^{i\mu\xi + \omega\tau}$$

$$H_1(\xi,\tau) = H^* e^{i\mu\xi + \omega\tau}$$

are used, $\mathcal{C}_0(\zeta)$ is given by Eq. 9, and ϵ is a small perturbation parameter. Note that in the moving coordinate system $H_0 = 0$.

The methodology of the LSA is explained in more detail in Viljoen et al. (1994), and we will only present the results here. The LSA yields the dispersion relation

$$\omega = -Pe - \frac{\phi}{Pe}\mu^4 + \frac{(\psi_2 - \psi_1\varphi)(Pe + \eta Da - \mu^2)}{(\psi_2 - \psi_1\varphi - \eta Da(1-\varphi))}, \tag{16}$$

where

$$\psi_{1,2} = \frac{1}{2}\left[-Pe \pm \sqrt{Pe^2 + 4(\omega Pe + \mu^2)}\right],$$

$$\varphi = \exp\left(\frac{\psi_2 - \psi_1}{\eta}\right).$$

The dispersion relation is an expression of the eigenvalue ω as a nonlinear function of the wavenumber of perturbation, μ, and various system parameters. The wave number μ is related to the wavelength of perturbation through $\lambda = 2\pi/\mu$. Growth of the planar interface is stable or unstable depending on the value of ω. If $\omega > 0$ for specific reactor conditions, any perturbation of the surface will grow, and if $\omega < 0$, perturbations will disappear and the planar surface will be the stable mode of propagation. Neutral stability is where $\omega = 0$, and conditions that lead to this situation are called critical conditions, since it represents the boundary between stable and unstable regions. Thus, for a specific set of conditions a critical wavenumber of perturbation, λ_{cr}, can be determined. If the planar interface is perturbed with a wavelength larger than λ_{cr}, the perturbation will grow in time and the planar interface is not a stable solution for those reactor conditions. On the other hand, all perturbations with wavelengths smaller than λ_{cr} will dissipate. By determining the critical wavelength at different substrate temperatures, pressures, and so forth, the dispersion relation enables us to study the effect of reactor conditions on the stability of planar film growth.

The dispersion relation (Eq. 16) is not in a very convenient form, though. Ideally, we want to express the eigenvalue ω as a polynomial function of the wavenumber. Let us try to simplify the dispersion relation. Consider the relative magnitude

of different parameters. Since convection effects as a result of movement of the interface are so small, $Pe \ll 1$. If short wavelength perturbations are most important, then $\mu^2 \gg Pe\omega$ and $\mu \gg Pe$. Therefore, $\psi_2 \approx -\mu$ and $\psi_1 \approx +\mu$. Furthermore, since η is very small and μ relatively large, it means that $\varphi \approx 0$. The dispersion relation becomes

$$\omega = -Pe - \frac{\phi}{Pe}\mu^4 + \frac{\mu(Pe + \eta Da - \mu^2)}{(\mu + \eta Da)}.$$

This relation can be simplified further if the relative magnitude of μ and ηDa is considered. If $\mu \ll \eta Da$, then

$$\omega \approx -Pe + \left(\frac{Pe + \eta Da}{\eta Da}\right)\mu - \left(\frac{1}{\eta Da}\right)\mu^3 - \left(\frac{\phi}{Pe}\right)\mu^4. \quad (17)$$

In most cases, however, $\mu \gg \eta Da$, which means

$$\omega \approx \eta Da - \mu^2 - \left(\frac{\phi}{Pe}\right)\mu^4. \quad (18)$$

This simplified dispersion relation clearly shows the effect of different parameters on the stability of planar growth. An increase in the Damköhler number increases the value of ω, which relates to a decrease in planar film stability. On the other hand, surface diffusion, as represented by the parameter ϕ, stabilizes planar growth, especially for small wavelength perturbations (where μ is large). Curves of ω as a function of μ from the biquadratic function in Eq. 18 in Figure 2 illustrate these trends. The critical wavelength, λ_{cr}, can be determined from the dispersion relation by noting that $\lambda_{cr} = 2\pi/\mu_{cr}$. For the simplified dispersion relation (Eq. 18),

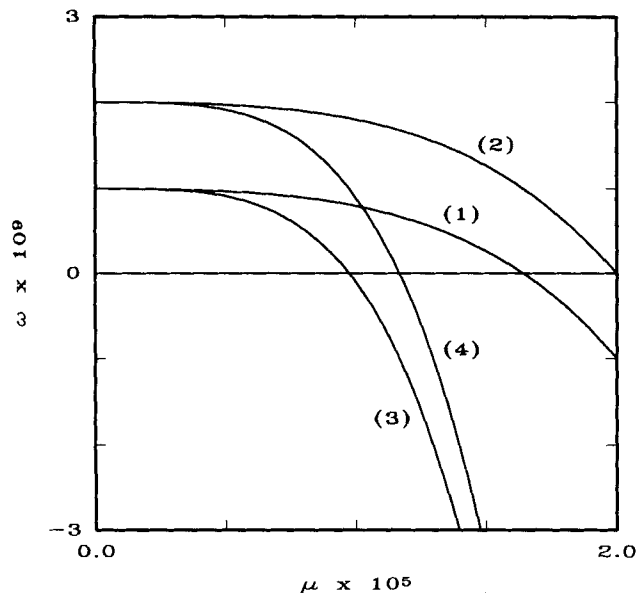

Figure 2. Effect of ηDa and ϕ/Pe on linear stability for simplified dispersion relation.

(1) $\eta Da = 10^{-9}$, $\phi/Pe = 10^{10}$; (2) $\eta Da = 2\times10^{-9}$, $\phi/Pe = 10^{10}$; (3) $\eta Da = 10^{-9}$, $\phi/Pe = 10^{11}$; (4) $\eta Da = 2\times10^{-9}$, $\phi/Pe = 10^{11}$.

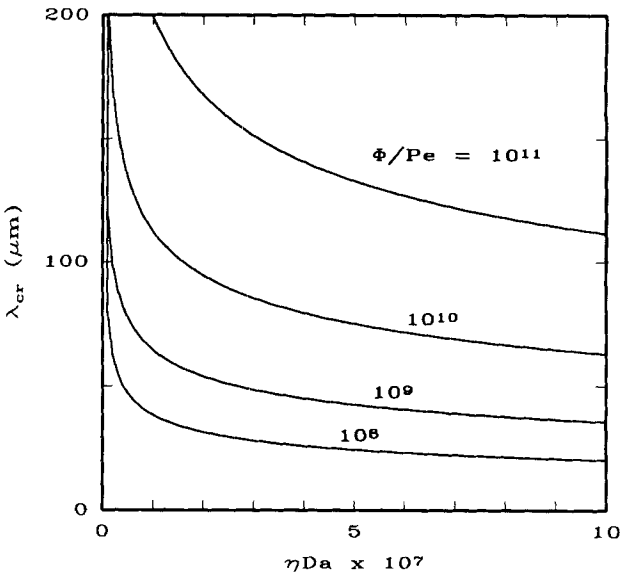

Figure 3. Effect of ηDa on critical wavelength, λ_{cr}, according to simplified dispersion relation and for different values of ϕ/Pe.

this value can be determined analytically:

$$\lambda_{cr} = \frac{2\pi}{\sqrt{\frac{Pe}{2\phi}\left[-1 + \sqrt{1 + 4\frac{\eta Da\,\phi}{Pe}}\right]}}.$$

This relation is shown in Figure 3 for different values of ϕ/Pe. The curves represent the boundary between stable (below lines) and unstable (above lines) regions. Note that the critical wavelength decreases with ηDa and increases with ϕ/Pe.

These results are valid only for cases where $\mu \gg \eta Da$. In general, the full dispersion relation, Eq. 16, should be used for studying stability effects. By considering the temperature dependence of material properties and therefore parameters such as ϕ, ηDa, and Pe, one can use the dispersion relation to determine the effect of temperature (or pressure) on the stability of planar film growth. This can be expressed in terms of the change in critical wavelength with temperature or pressure, or one can determine the change in maximum allowable bulk concentration that will ensure planar film growth for a specific size perturbation (Viljoen et al., 1994).

Now consider a specific example, with the choice of parameters as in Table 3. Important information can be obtained from the planar solution and the LSA without having to solve the complete system of PDEs. For specific reactor conditions

Table 3. Parameters and Constants for Typical CVD Process

Parameter	Value	Parameter	Value
P (atm)	1.0	K_3 (m^2/s)	10^{10}
% dilution	95	K_4	1.823
δ (m)	10^{-3}	K_5 (m^3/s)	2×10^{-5}
K_1 (m/s)	10^7	K_6 (kcal/mol)	87.4
K_2 (kcal/mol)	47.7	K_7 (mK)	8×10^{-9}

Table 4. Effect of Temperature on Growth Rate and Planar Film Stability for Choice of Parameters in Table 3

T (K)	Growth Rate (μm/h)	C/C_b at Interface	Da	ϕ	λ_{cr} (μm)	λ_m (μm)	t_d (min)
1,000	2.06	0.987	0.0128	6.61×10^{-6}	8.08	359	1.57×10^{6}
1,200	63.3	0.666	0.502	8.70×10^{-3}	7.30	43.6	1,320
1,400	187	0.132	6.60	1.44	10.4	34.5	35.3
1,600	235	0.0222	44.1	65.7	16.2	35.3	5.28
1,800	263	5.28×10^{-3}	188	1.26×10^{3}	25.6	45.0	2.29
2,000	288	1.69×10^{-3}	590	1.34×10^{4}	44.1	71.8	2.41

(temperature and pressure), reactant concentration at the interface is given by Eq. 11, and the deposition rate is determined by solving Eq. 10. System parameters and stability results are presented in Table 4 for a range of temperatures. Note how the growth rate increases with temperature, and the reactant concentration (C/C_b) at the interface decreases sharply. At low temperatures it almost equals its value in the bulk, which indicates there are no significant mass-transfer limitations and the process is controlled by surface kinetics. With an increase in temperature the kinetics become faster and interface concentration decreases to a point where the process becomes controlled by diffusion in the gas phase. This is confirmed by plotting the logarithm of deposition rate as a function of the reciprocal of temperature (Figure 4). A shift in controlling mechanism occurs where the slope of the curve changes. It shows that we can identify three regions: the kinetic, transition, and diffusion-limited regimes. The process is in the kinetic regime at relatively low temperatures (up to ~ 1,100 K), which corresponds to small values of the Damköhler number ($Da < 0.1$). With an increase in temperature, a transition from kinetic to diffusion-limited growth takes place ($0.1 < Da < 10.0$). At high temperatures (higher than ~ 1,440 K) the process is severely mass-transfer-limited, thus for values of the Damköhler number larger than ~ 10.

Table 4 also shows the effect of temperature on the stability of planar growth. The critical wavelength (λ_{cr}) is obtained by solving the dispersion relation (Eq. 16) for $\omega = 0$ under specific conditions, for example, specific temperature. This represents the boundary between stable and unstable regions. Therefore, a protrusion with wavelength smaller than λ_{cr} will be smoothed, while one larger than λ_{cr} will grow unstably. The critical wavelength decreases with temperature, reaches a minimum, and then increases again. This trend is shown in Figure 5. The reason for the minimum lies in the difference between activation energies for the surface reaction and surface diffusion. The latter is larger and the stabilizing effect of surface diffusion becomes significant only at high temperatures. This is evidenced by the large increase in the value of ϕ as shown in Table 4.

The *most* unstable wavelength λ_m can also be determined from the dispersion relation. It is the wavelength that corresponds to the largest value of the eigenvalue ω and represents the wavelength of perturbation that will grow fastest and dominate during the initial stages of unstable growth. The value of λ_m is important when choosing a physically meaningful size of substrate to simulate numerically. Usually, the substrate to be considered is chosen much larger than λ_m to ensure that end effects do not affect the natural development of interface shapes. Another important parameter in

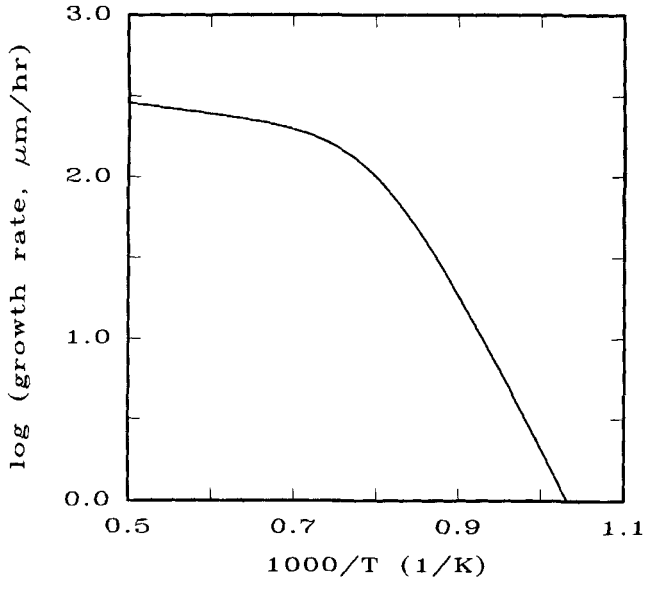

Figure 4. Effect of temperature on growth rate showing shift in controlling mechanism.

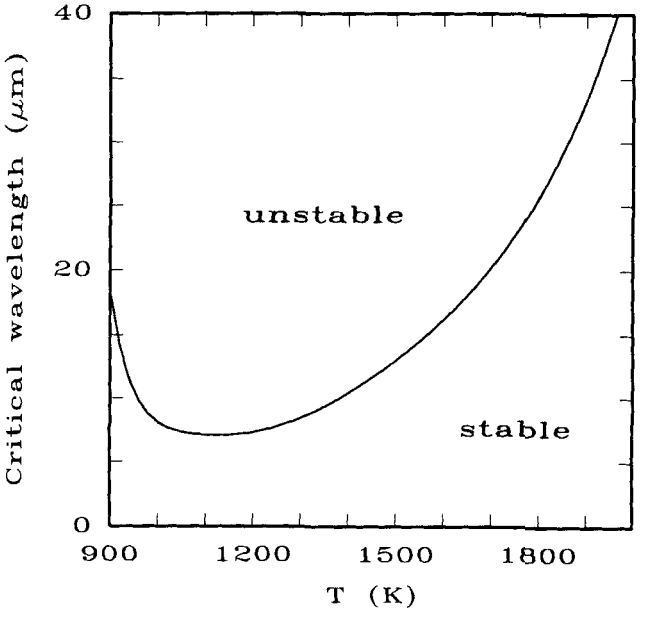

Figure 5. Effect of temperature on critical wavelength for parameters in Table 3.

Table 4 is t_d. This value represents the deposition time necessary to double the amplitude of the most unstable perturbation (with wavelength λ_m) and therefore gives a good indication of the time scale of unstable growth. It is determined from the time dependence of the perturbed solution, thus from $2 = \exp[\omega_m t_d]$, where ω_m is the eigenvalue corresponding to the *most* unstable wavelength, λ_m. For example, for the set of chosen parameters, at 1,200 K it would take 22 h to double the amplitude of perturbations (around 1 μm), while the film thickness at this time would already be 1,400 μm. This means that even under unstable planar growth conditions, you may not see significant film nonuniformity, unless a film of several *millimeters* is grown. However, at 1,600 K the value of t_d is down to only 5.3 min, which means very severe nonuniformities can be expected even at short deposition times.

Numerical Solution of Governing Equations

Even though the LSA yields valuable information about stability of the basic solution (in our case the planar interface), it does not predict the form of interface evolution for general conditions significantly different from those required for planar growth. This information can be obtained only from solving the governing equations and following the evolution of the interface with time. The system of equations represents a coupled nonlinear initial-boundary value problem that cannot be solved analytically for general conditions. The problem is further complicated by the presence of an interface with arbitrary shape, or free boundary. However, it is possible to make assumptions that can simplify the problem significantly. For example, from a time-scale analysis we can determine that changes in the gas phase take place much faster than the time scale of solid film growth (Thiart et al., 1994). Therefore, the gas phase problem can be considered in pseudo-steady state with respect to changes in the solid phase. This means the problem can be solved on the solid phase time scale, with the gas phase equations solved in steady state and independently at each instant in time. Essentially, this decouples the two phases and they are solved successively at each time step rather than simultaneously.

Simplified solution

The determination of the concentration field is the most time-consuming step in the numerical procedure, since the computational domain is *one* dimension larger than that for the interface. In the present study the interface is represented by a line (thus 1-D), and the gas phase is the 2-D domain above it. Determination of the gas phase solution is therefore computationally much more demanding than that for the interface shape. This will be even more true when a 2-D interface is considered with a 3-D gas phase problem. It is therefore very helpful to find an approximate solution to the gas phase equations and simplify the problem to solving the interface evolution equation only. Let us consider possible simplifications.

An assumption that is reasonable in many cases is that there are no sharp gradients in the interface, and it is assumed to be fairly close to planar form. That means we can use the model formulation as represented by Eqs. 12 to 15. Now consider two limiting cases of deposition control.

Diffusion-limited

A previous study has shown that the reactant concentration at the interface under diffusion-limited growth conditions will be close to *zero* and will be approximately proportional to the height of the interface (Thiart et al., 1994). Therefore, approximate the gas concentration at the interface as its value at that height above a planar interface. Thus, from Eq. 9

$$\mathcal{C}|_{\zeta=H} = \frac{1}{\beta C_b}\left[\left(\frac{Pe+\eta Da}{\eta Da}\right) - \exp(-PeH)\right]. \quad (19)$$

This decouples the gas and solid phase problems, and the equation for interface evolution becomes

$$\frac{\partial H}{\partial \tau} = \frac{\eta Da}{Pe}\left[\left(\frac{Pe+\eta Da}{\eta Da}\right) - \exp(-PeH)\right][1+\kappa]\sqrt{1+H_\xi^2} - 1 - \frac{\phi}{Pe}\left[\frac{\kappa_\xi}{\sqrt{1+H_\xi^2}}\right]_\xi$$

For most physical cases $PeH \ll 1$, thus $\exp(-PeH) \approx 1 - PeH$, which when substituted into the growth equation leads to

$$\frac{\partial H}{\partial \tau} = (1+\eta DaH)(1+\kappa)\sqrt{1+H_\xi^2} - 1 - \frac{\phi}{Pe}\left[\frac{\kappa_\xi}{\sqrt{1+H_\xi^2}}\right]_\xi.$$

Now consider the weakly nonlinear form where $|H_\xi| \ll 1$, in which case $\sqrt{1+H_\xi^2} \approx 1 + \frac{1}{2}H_\xi^2$. The equation for interface evolution becomes

$$H_\tau = \eta DaH + \frac{1}{2}H_\xi^2 + H_{\xi\xi} - \frac{\phi}{Pe}H_{\xi\xi\xi\xi} \quad (20)$$

with periodic boundary conditions

$$H(0,\tau) = H(nl/\Gamma,\tau),$$
$$H_\xi(0,\tau) = H_\xi(nl/\Gamma,\tau),$$
$$H_{\xi\xi}(0,\tau) = H_{\xi\xi}(nl/\Gamma,\tau),$$
$$H_{\xi\xi\xi}(0,\tau) = H_{\xi\xi\xi}(nl/\Gamma,\tau),$$
$$\text{with} \quad n = 0, \pm 1, \pm 2, \ldots, \quad (21)$$

and with initial condition

$$H(\xi,0) = \mathcal{H}_0(\xi), \quad (22)$$

where $\mathcal{H}_0(\xi)$ is an arbitrary initial interface shape.

The growth equation is still a nonlinear PDE, but it is in a form suitable for application of standard numerical techniques, and is much simpler to solve than the original system of coupled equations. If a linear stability analysis of the simplified equation is performed, we find a very interesting re-

sult: The dispersion relation is identical to the simplified dispersion relation for the complete system, thus Eq. 18. This means the simplified equation has the same linear stability behavior as the original system (when $\mu \gg \eta Da$) and confirms the validity of the assumption used to arrive at Eq. 20. The dispersion relation therefore has the form

$$\omega = \eta Da - \mu^2 - \left(\frac{\phi}{Pe}\right)\mu^4. \tag{23}$$

Kinetic control

Another limiting case is deposition under kinetic control. The interface concentration will be close to that in the bulk gas and can therefore be assumed as constant. Let us assume it to be the value at the interface under planar deposition conditions. This is given by Eq. 11. The weakly nonlinear form of the growth equation becomes

$$H_\tau = \frac{1}{2}H_\xi^2 + H_{\xi\xi} - \frac{\phi}{Pe}H_{\xi\xi\xi\xi} \tag{24}$$

with the same boundary and initial conditions as Eq. 20. This equation is identical to Eq. 20 except for the absence of the destabilizing term ηDaH, which accounts for preferential growth of protrusions relative to depressions. Predictably, the linear stability of Eq. 24 shows that planar growth is inherently stable for all wavelengths of perturbation.

Solving Eqs. 20 and 24 shows us more about interface evolution than the LSA of the full system does and therefore brings us a step closer to visualizing interface behavior in the real system. However, these equations are strictly valid only for interface shapes close to planar, and are therefore also limited in their application.

Solution of complete system

Numerical techniques for solving this kind of problem can be divided into two classes: the first is where interface shape and the field variable are decoupled and solved with successive approximation, and the second is simultaneous iteration for interface shape and field variables. Another distinction between different methods concerns the solution domain. One option is to transform the original coordinate system onto a domain with fixed boundaries, of which the interface is one. Grid or mesh generation is then simple, but the field equations become more complex. Alternatively, the problem can be solved in the original coordinates, where the grid or mesh changes with time. Generation of a new irregular mesh at each iteration becomes necessary. Ettouney and Brown (1983) evaluated different numerical techniques and found that the Galerkin finite element technique was well-suited to solving steady solidification problems. They preferred solution of the problem in transformed coordinates, and studied cases where the interface could always be expressed as a single-valued function of the horizontal coordinate. For more complex interface shapes the transformation between the regular and computational domain could be more difficult.

In a previous study, the full system of equations was solved numerically for a variety of deposition conditions by considering interface evolution in terms of vertical displacement and using the conventional Cartesian coordinate system (Thiart et al., 1994). The position of the interface was expressed as a single-valued function of the horizontal coordinate ($H(\xi)$). Thus interface curves were expressed in terms of the gradient $\partial H/\partial\xi$. The gas and solid phase problems were decoupled by solving them successively at each instant. Satisfactory results were obtained for cases where deposition was not severely diffusion-limited, thus where $Da < 10$. In these cases, interface gradients ($\partial H/\partial\xi$) remained finite. However, there were many physically meaningful cases where gradients approached infinity and resulted in breakdown of the numerical procedure. The conventional Cartesian coordinate system, where the interface position was expressed as a single-valued function of the horizontal coordinate, became inappropriate, because it limited the natural evolution of highly irregular interface shapes.

Choice of appropriate parametrization

The position of interface was expressed as a function of a parameter, say σ, which was chosen as the horizontal coordinate x (or ξ) for representation in the Cartesian coordinate system. However, this choice of parameter proved inappropriate for cases where significant mass-transfer limitations were present. In the present study we use a more appropriate choice of parameter, which will permit the evolution of any possible interface shape. For initial or boundary value problems where steep gradients and large curvature are encountered, for example, in flame and combustion problems, the so-called *arc-length strategy* has typically been used. In this technique, a function such as position of the interface, is not expressed in terms of the horizontal coordinate, since this can lead to problems in regions of steep gradients. Instead, the function is expressed in terms of its change along the arc length of the curve, which stretches the curve and eliminates steep gradients. A multivalued function in the horizontal coordinate becomes a single-valued function in the arc length of the curve. Therefore, the arc length (say s) is introduced as new independent variable and the original independent variable (say x) becomes a dependent variable. The relation between x and s introduces an additional equation, and the original system equations are transformed and expressed in terms of the arc length s (Bhatia and Hlavacek, 1983; Kubicek, 1976). The problem is solved in terms of the new parameter s, which proves computationally more convenient in the region of steep gradients than the original system. The method has proved to be a very useful tool in continuation methods and for tracing solution branches in bifurcation diagrams (Seydel and Hlavacek, 1987).

The arc length seems the obvious choice as a parameter for expressing the position of an interface during CVD growth. However, in the present initial-boundary-value problem it has the disadvantage that the total arc length changes with time and its value at each point in time is not known *a priori*. This introduces an unnecessary complication to the solution procedure. An appropriate choice of parameter is one that has a fixed total length not dependent on time, and that can be discretized into an equidistant grid. The *normalized* arc length satisfies all the requirements set for an appropriate parameter, since its range is constant and known *a priori* (it is chosen arbitrarily), and the position of the interface is a unique function of σ. This means that the gradients $\partial x/\partial\sigma$

and $\partial z/\partial\sigma$ cannot approach infinity as in the former case where σ was chosen as x (or ξ). The relation between σ and the position of the interface is not an analytical function, but this is not necessary. The interface is discretized into an equidistant grid with predetermined number of points, and spatial derivatives at each point are represented by appropriate finite difference formulas. Interface position is therefore known at discrete values of the parameter.

The numerical solution is therefore obtained in the following way: the gas and solid phase equations are decoupled by solving them successively at each instant, instead of simultaneously. An explicit method is used, which eliminates the need for iterative solution, but this means that extremely small time steps are required to ensure stability of the finite difference scheme. The equation for interface evolution is expressed in terms of the parameter σ (normalized arc length) and solved by finite differences on an equidistant grid in σ. The gas phase equations are solved by Galerkin finite elements in the original Cartesian coordinate system and with the interface shape as input at each time step. This requires the automatic generation of a 2-D mesh with irregular and changing boundaries at each time step.

Automatic mesh generation

In most problems with steep gradients, the mesh is generated once only at the start of the solution procedure. However, in the solution of a free-boundary problem, the mesh changes constantly as the interface changes shape, and therefore has to be generated at each point. This step can be very time-consuming and it is therefore necessary to use an efficient automatic mesh-generation scheme. For an accurate numerical solution in the gas phase, it is necessary to place nodes in the 2-D gas domain in such a way that the resulting quadrilateral cells have appropriate shapes. They should be as close as possible to rectangles (no angles close to 0° or 180°) with aspect ratios preferably smaller than 10 to 1, to ensure an accurate Galerkin finite element representation. Accordingly, one can define three optimization criteria for placement of interior points: adaption, smoothness, and orthogonality. The first criterion refers to concentrating nodes in specific regions inside the domain, for example, close to one of the boundaries. This is done to ensure sufficient resolution in areas where severe changes or steep gradients are anticipated, such as is the case in combustion problems (Degreve et al., 1987). In the present study the gas concentration close to the interface is important for determining interface dynamics and it is desirable to concentrate nodes close to this boundary. In addition, the number of points along the interface is typically much larger than that in the vertical direction (up to 10 to 1), which means strong adaption is necessary at the interface to ensure acceptable aspect ratios of elements in that region. Smoothness refers to the requirement that there should be a gradual change in cell size, since any rapid variations lead to inaccuracies (Thompson et al., 1985). The orthogonality criterion strives to make all cell angles 90°, which is desired for sufficient solution accuracy.

In determining the position of interior nodes, the mesh-generation scheme optimizes measurable quantities of these three criteria, expressed in terms of the positions of nodes. However, the three criteria are essentially noncomparable, which leads to a complex vector optimization problem. One way to deal with this problem is to assign different scalar weights to each criterion, depending on its importance, and to combine them into one objective function. The procedure is essentially a discrete version of the variational method proposed by Brackbill and Saltzmann (1982). More details are given in Degreve (1990).

To illustrate the use of our automatic mesh generator, and to show the effect of adaption and orthogonality, consider the two meshes in Figure 6. An arbitrary interface shape was chosen (it does not have to be symmetrical) and the position of interior nodes on a 50×20 element mesh were determined. In both cases the position of points was adapted to be more concentrated near the interface. In the first mesh (Figure 6a), the weights for adaption and orthogonality were similar and relatively small, and the result is a very uniform mesh.

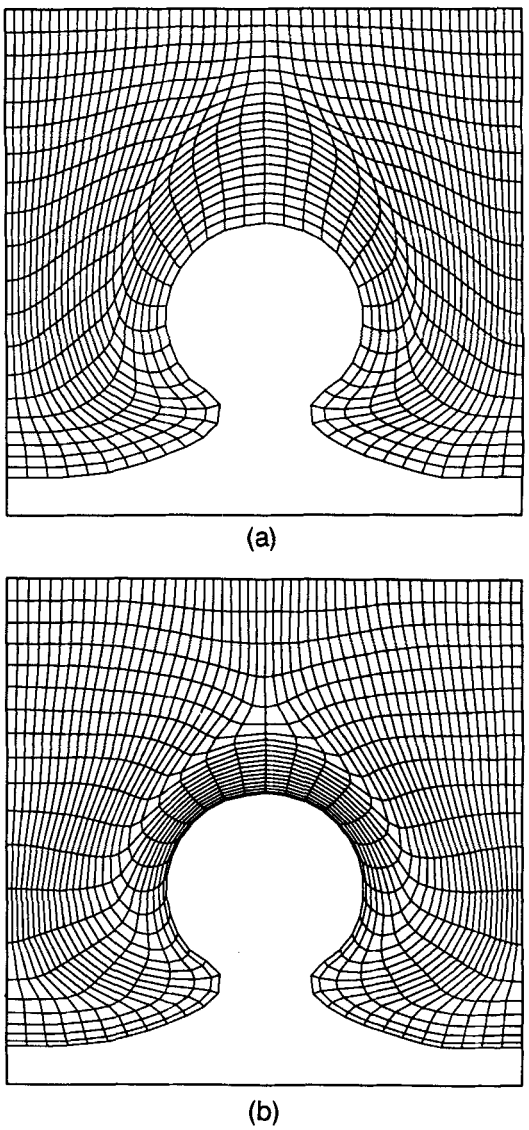

Figure 6. Examples of meshes from automatic mesh generator.

(a) Relatively uniform cells and small aspect ratios with little emphasis on adaption or orthogonality. (b) Adaption close to bottom boundary and larger weights of orthogonality result in better cell orthogonality, but aspect ratios increase.

In the second mesh (Figure 6b), both orthogonality and adaption were increased and as a result cells are more rectangular in shape, but their aspect ratios have increased. The relative weighting of adaption, orthogonality, and smoothness therefore have to be tailored to the requirements of the specific case under consideration.

Numerical Examples

Application of the solution procedure outlined earlier can be illustrated through numerical examples of CVD growth from arbitrary initial interface shapes for any desired deposition time. Since periodic boundary conditions are applied, the interface length to be simulated can be chosen arbitrarily. However, it is important to consider a sufficiently large part of the substrate to avoid the influence of end effects. Generally, the horizontal range is chosen between 5 and 20 times that of the critical wavelength, λ_{cr}.

As a first example, consider growth from two randomly rough initial conditions, similar to what may be expected in practical applications. We use the parameters as given in Table 3. The results are shown in Figure 7 for increasing temperatures, which correspond to increasing values of the Damköhler number, *Da*. Since growth rates change significantly with temperature, different deposition times were chosen to ensure approximately the same final film thickness. The results clearly show that deposition is very uniform at low temperature (~ 1,100 K), but becomes much less uniform as deposition temperature is increased, and becomes fingerlike at high temperature. This trend has also been observed experimentally, for example, in the CVD growth of Si from $SiHCl_3$ (Van den Brekel, 1977) and the deposition of CrB_2 from CrO_2Cl_2 and BCl_3 (Schmidt, 1991). The fingerlike growth can be attributed mainly to different controlling mechanisms of deposition. At low temperature (~ 1,100 K), the process is controlled by surface kinetics ($Da < 1$), and reactant concentration is approximately constant over all parts of the film surface. However, as temperature increases, diffusional limitations develop (as evidenced by increase in *Da*) and reactant concentration in depressions becomes depleted relative to that at protrusions. The result is a very nonuniform fingerlike structure. The results in Table 4 indicate that

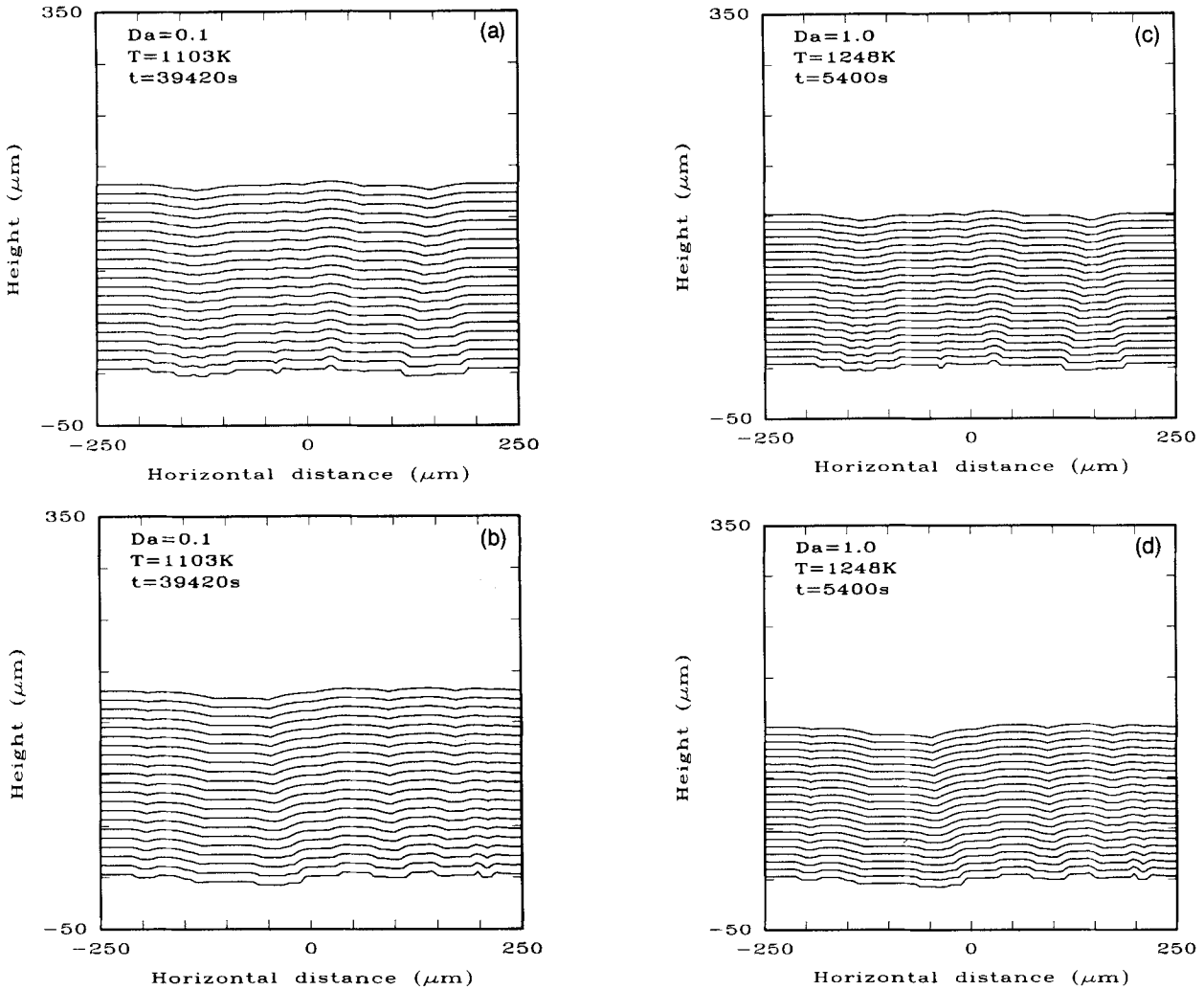

Figure 7. Effect of temperature and thus Damköhler number on uniformity of film growth from two randomly rough initial interfaces at a constant pressure of 1 atm.

(a), (b) $Da = 0.1$; (c), (d) $Da = 1.0$.

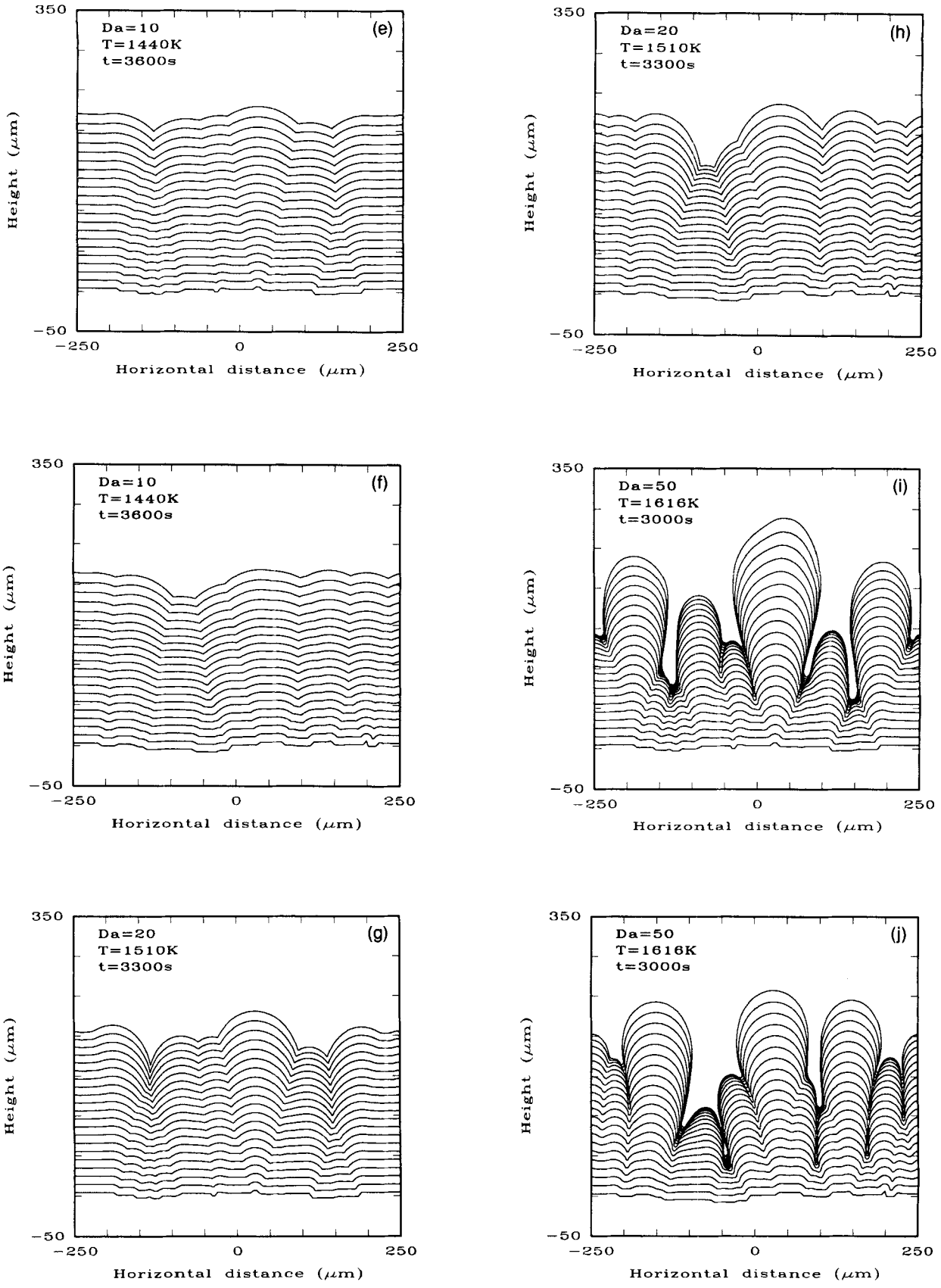

Figure 7. Effect of temperature and thus Damköhler number on uniformity of film growth from two randomly rough initial interfaces at a constant pressure of 1 atm.

(e), (f) $Da = 10$; (g), (h) $Da = 20$; (i), (j) $Da = 50$.

the effect of surface diffusion becomes very strong with increasing temperature (as evidenced by the large increase in ϕ), and one would therefore expect surface diffusion to limit the growth of fingers and prevent the formation of deep grooves, but this is not the case. The reason lies in the magnitude of interface curvature. Surface diffusion is effective only for very high curvature and therefore over short wavelengths. Protrusions in the specific examples considered have relatively large wavelengths and the effect of surface diffusion is therefore overshadowed by the destabilizing effect of gas diffusional limitations.

Another experimentally observed phenomenon that is shown by the results in Figure 7 is the tendency of some fingers to nose ahead of their neighbors. This is the result of depletion of reactant in the grooves between large fingers. An interesting phenomenon is the tendency of some grooves to close and form occlusions, while others remain open. Numerically, this is taken care of by eliminating all parts of the interface that overlap, and rearranging points on the remaining part. The formation of occlusions contributes to film porosity and has an adverse effect on film properties. One should note, however, that the model is strictly valid only for cases where the MFP is much shorter than the width of a groove. Just before grooves "neck off," this restriction is violated and Knudsen diffusion is a more appropriate transport mechanism. However, this effect is not expected to change the quality of results significantly. The results in Figure 7 illustrate the limitations of a model where interface shape is represented as a single-valued function of the horizontal coordinate. Such a model cannot predict the formation of occlusions, which is an important physical phenomenon, or the nonvertical growth of grooves.

Figure 8 shows isoconcentration lines at the end of the runs for deposition cases in Figures 7a and 7i. The results in Figure 8a indicate that reactant concentration at the interface is fairly close to its value in the bulk under kinetically controlled deposition ($Da = 0.1$). It is also fairly constant and varies less than 0.1% with position along the interface. Under diffusion-limited conditions ($Da = 50$), however, reactant concentration at the interface changes significantly with position and there is a 500% increase in the concentration from the base to the top of the largest finger. Also note that there is a large difference in the magnitude of interface concentration in kinetic and diffusion-limited cases. Reactant concentration at the interface is close to the bulk value for $Da = 0.1$ and close to zero for $Da = 50$. To illustrate the effect of the controlling mechanism on film growth more clearly, consider the following example. Suppose the final interface shape in Figure 7i is used as a new initial condition for film growth under kinetic control ($Da = 0.1$) and gas diffusional control ($Da = 50$). Let us consider the gas phase solution in these cases. Figures 9a and 9b shows the isoconcentration lines under kinetic and diffusional control, respectively. Under conditions of diffusion-limited growth, the isoconcentration lines tend to follow the shape of the interface. They are closer together above fingers and rarefied in grooves. Since growth is proportional to the concentration gradient, and the gradient is larger where isoconcentration lines are closer together, this clearly shows that preferential growth of fingers will take place under diffusion-limited conditions. However, under kinetic control the form of isoconcentration lines is reversed,

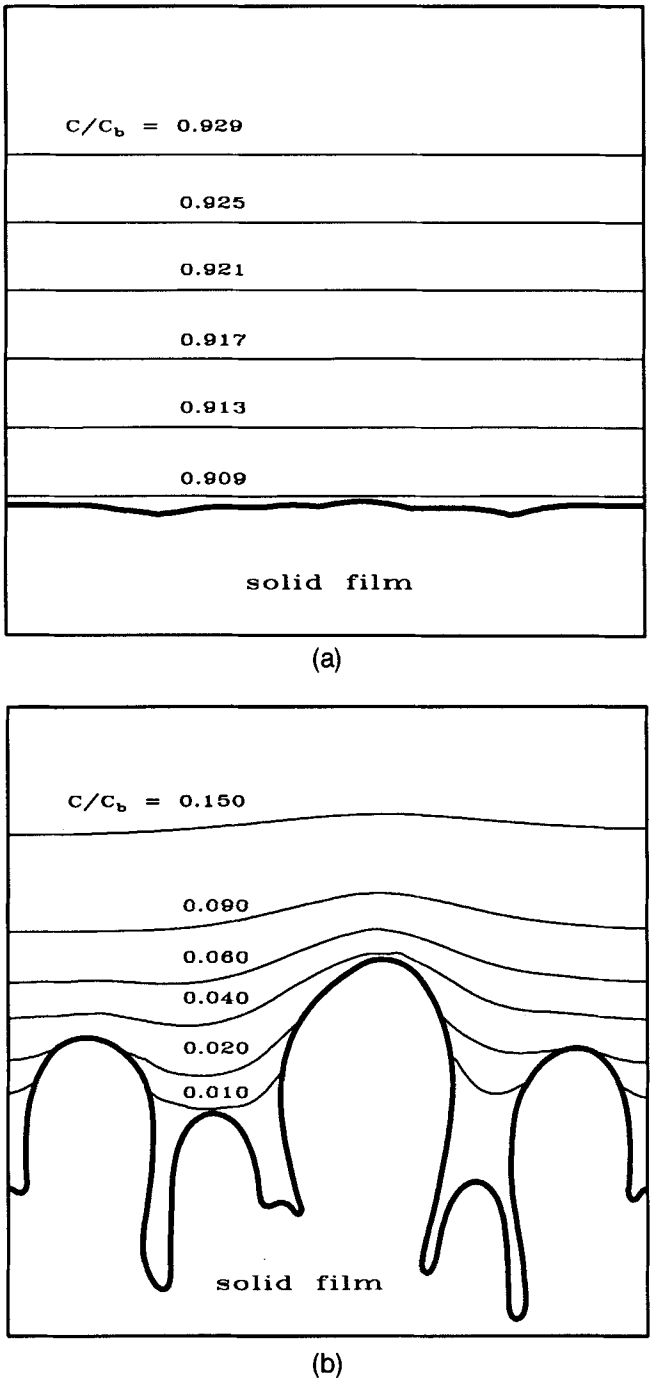

Figure 8. Isoconcentration lines in the gas boundary layer for deposition conditions in Figures 7a and 7i.

and they are rarefied above fingers and closer together in grooves. In this case, the form of isoconcentration lines compensates for the effect of interface curvature on reactant concentration, since reactant flux to all parts of the interface is almost the same. The results in Figures 10a and 10b show the different growth characteristics in the two cases. It shows interface evolution from the fingerlike initial shape for conditions as in Table 3 and for $T = 1{,}248$ K and $T = 1{,}616$ K, respectively. Under diffusional control, finger formation con-

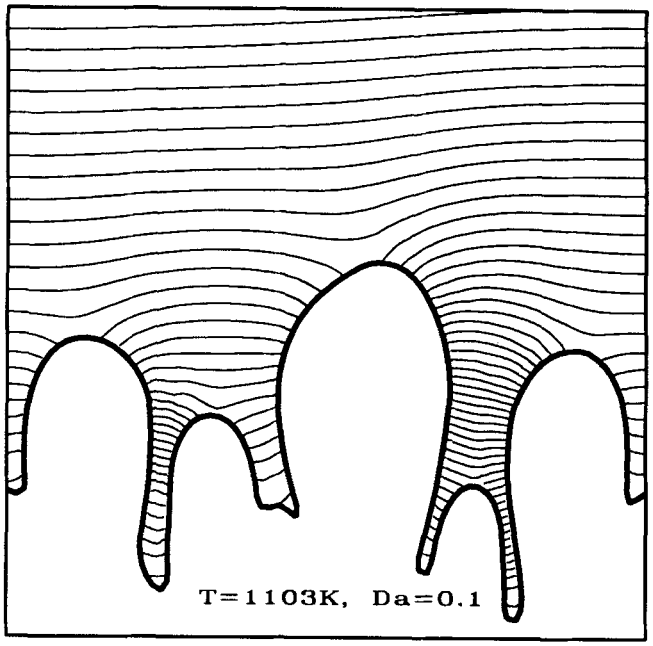

(a)

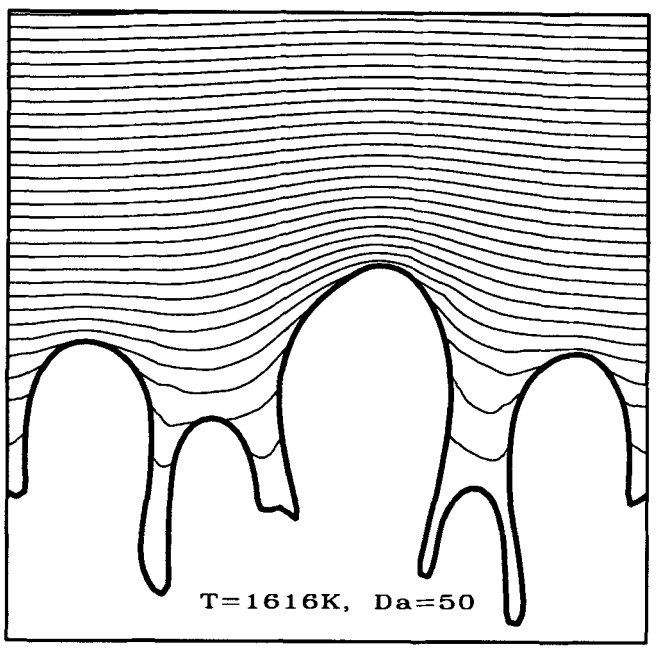

(b)

Figure 9. Isoconcentration lines for growth from finger-like initial condition under (a) kinetic control ($Da = 0.1$), and (b) diffusional control ($Da = 50$).

Different shape of isoconcentration lines illustrates reason for growth of protrusions.

tinues, but under kinetic control, grooves are filled and the relative height of fingers decrease. Note that the length of substrate considered in Figures 9 and 10 is identical to that in Figures 7 and 8.

A common experimental observation in film deposition is the tendency to form semicircular nodules, where some nodules increase and other diminish in size (Parretta et al., 1990; Messier and Yehoda, 1985; Messier, 1986). This *growth–death* phenomenon is the result of growth normal to the interface and a tendency to minimize surface energy. It seems most prevalent in our simulations for growth at moderate values of the Damköhler number ($Da \approx 20$), as can be seen from results in Figures 7g and 7h. This phenomenon can also be observed in our numerical simulations by following interface evolution from an initial condition where large irregularities are present, thus with severe roughness. Figure 11 shows the

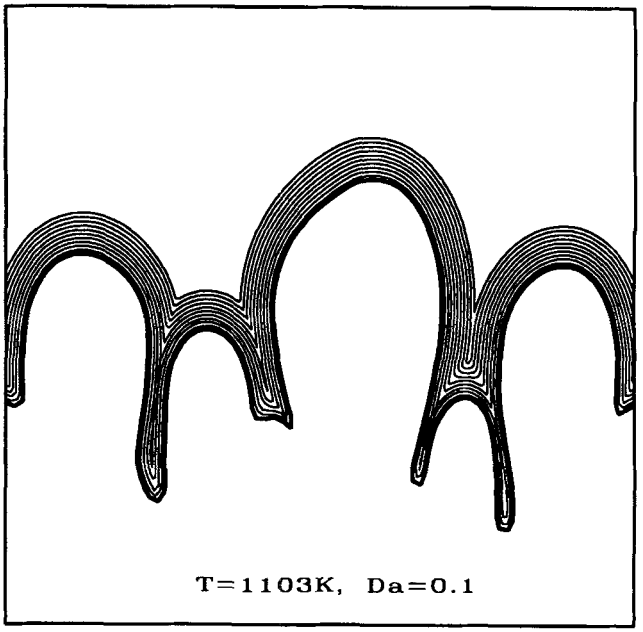

(a)

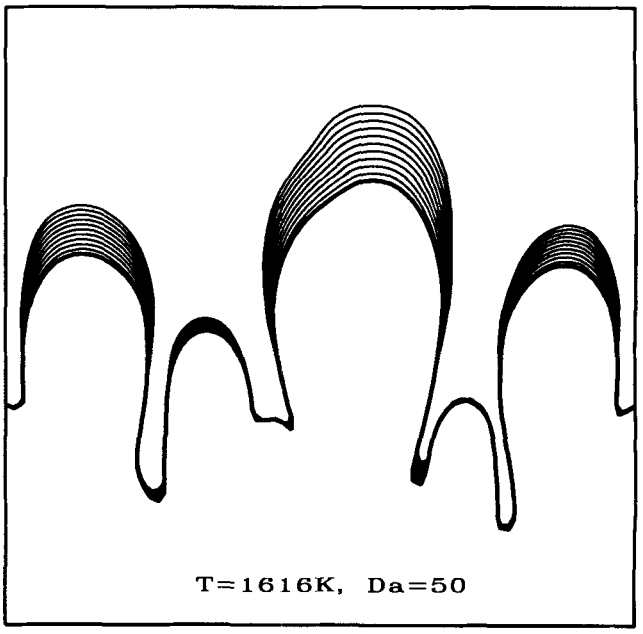

(b)

Figure 10. Film growth for conditions with isoconcentration lines as shown in Figure 9.

(a) Under kinetic control, $Da = 0.1$; (b) under diffusion-limited conditions, $Da = 50$.

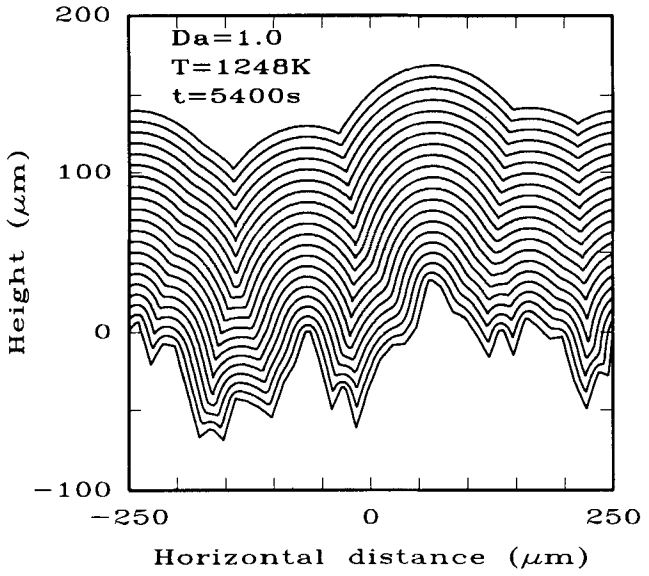

Figure 11. Development of semicircular cap structure showing growth–death phenomenon.

growth of a film at relatively low temperature (1,248 K) for the conditions as in Table 3. The results clearly show the semicircular structure and the tendency of some caps to increase in size while others disappear.

Reactor pressure is another deposition variable that affects film uniformity. Gas diffusivity is inversely proportional to reactor pressure, and therefore many CVD processes are conducted at reduced pressure to increase reactant diffusion to the interface. A decrease in operating pressure has been found to improve the stability of planar film growth (Viljoen et al., 1994; Ananth and Gill, 1992). Through the relation between pressure and diffusivity (D_f), the Damköhler number, Da, is proportional to reactor pressure. This means we should be able to reduce diffusional limitations by decreasing the deposition pressure. Figure 12 shows the effect of pressure on film growth at high deposition temperature (~ 1,600 K). Conditions were chosen identical to those in Figure 7i, except for the pressure. The results show that film uniformity can be improved significantly if the pressure is reduced from 1 to 0.1 atm. This decrease in pressure also corresponds to a decrease in the Damköhler number from $Da = 50$ to $Da = 5$.

The initial interface shape can be chosen arbitrarily in our numerical solution procedure. Let us repeat the runs in Figure 7, but for initial shapes of triangular V-grooves and rectangular trenches with a range of aspect ratios. These shapes are typically found in electronic applications, but note that the length and time scales may be completely different. Nevertheless, the results do show interesting growth phenomena similar to what is observed in electronic applications. Figures 13a to Figure 13h show the effect of temperature on the uniformity of film growth in three rectangular grooves and three V-grooves of different size. The rectangular grooves have aspect ratios of 1:1, 2:1, and 4:1. Once again, parameters were chosen to have the values indicated in Table 3 and reactor pressure was taken as atmospheric. The results show that all grooves are filled uniformly at low temperature (~ 1,100 K) and thus low values of Da. Therefore, good *step coverage* is obtained under these conditions. The term *step coverage* refers to the thickness of film inside the groove relative to that outside in regions without grooves (Oh et al., 1992). As the temperature is increased, occlusions start to form in all three rectangular grooves, and at $T = 1{,}616$ K severe finger formation has taken place. At this temperature almost no material has deposited in the grooves as a result of severe diffusional limitations. If this situation is undesirable, diffusional limitations can be reduced and step coverage therefore improved by decreasing reactor pressure. The results of film growth in V-grooves illustrate that the size of grooves is im-

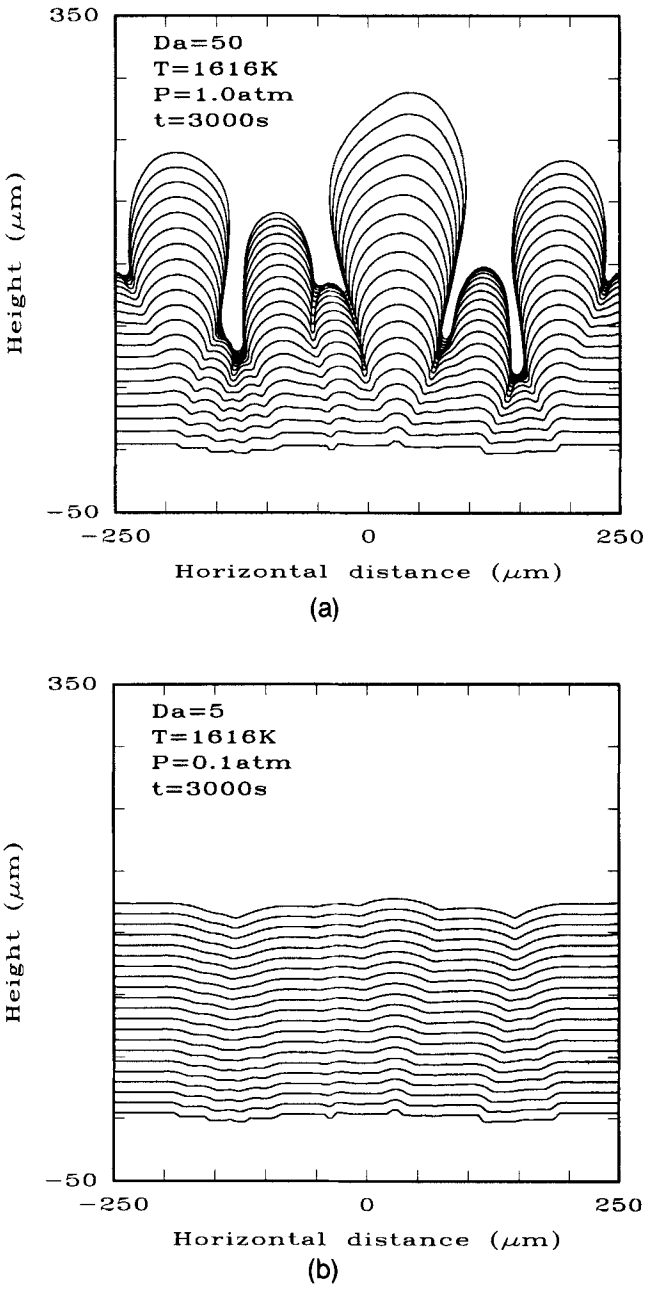

Figure 12. Effect of pressure on film uniformity at high temperature and for conditions as in Figure 7g.

(a) atm; (b) 0.1 atm.

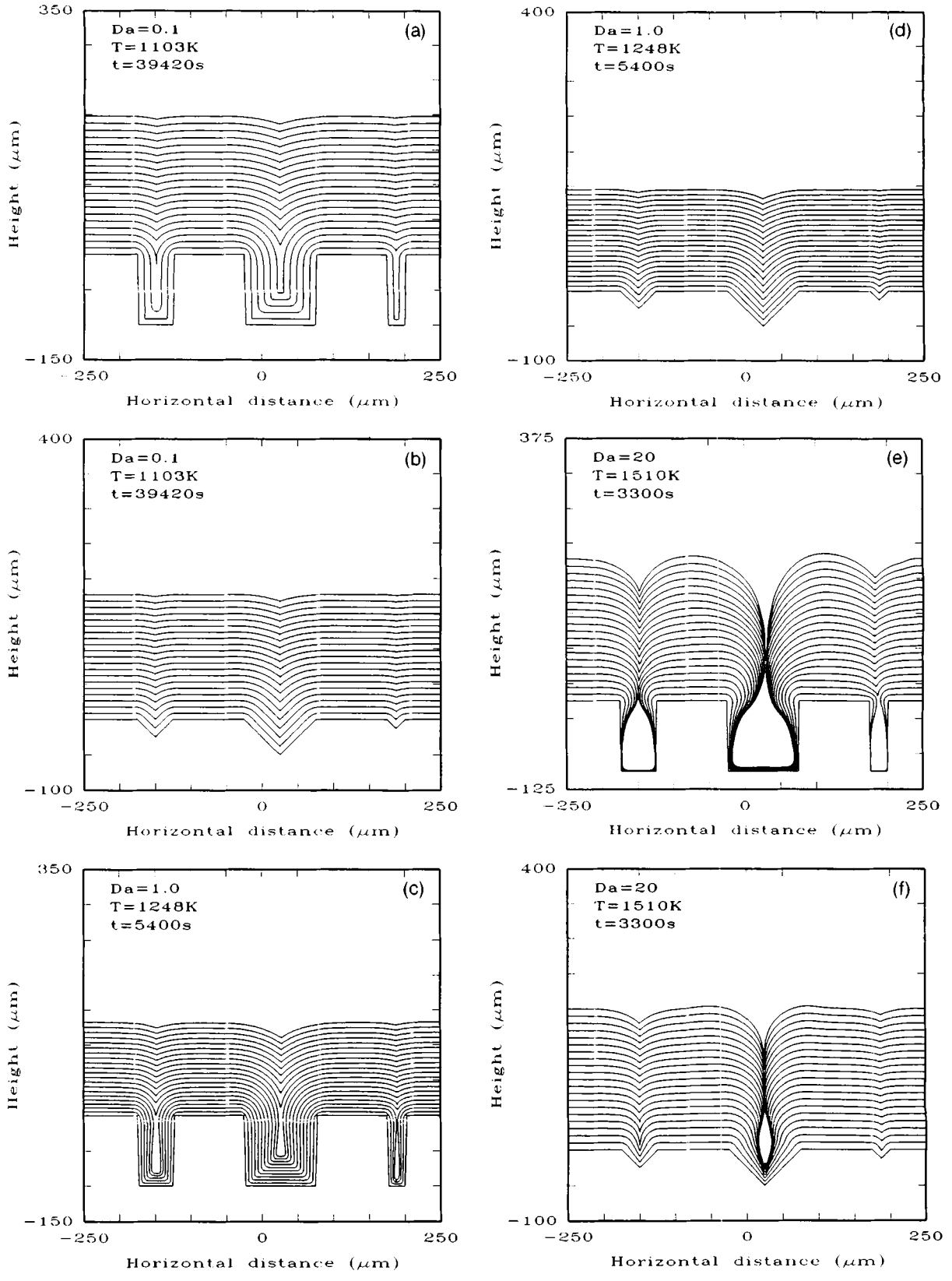

Figure 13. Effect of temperature and thus Damköhler number on uniformity of film growth in rectangular and V-shaped grooves at a constant pressure of 1 atm.

(a), (b) $Da = 0.1$; (c), (d) $Da = 1.0$; (e), (f) $Da = 20$.

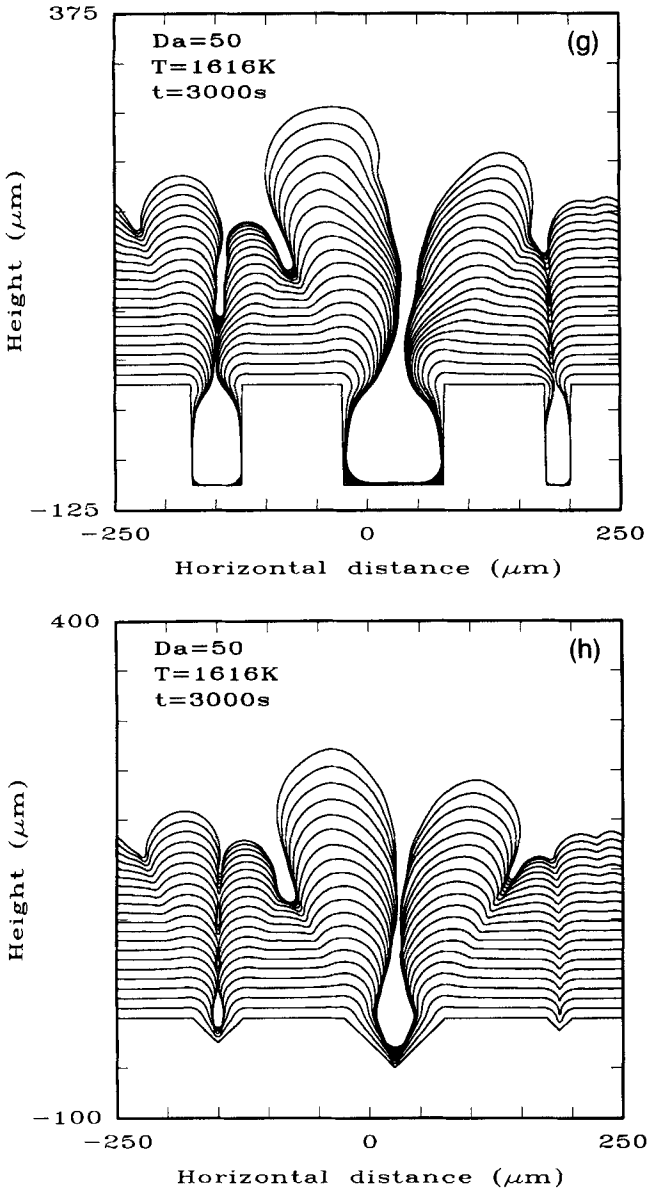

Figure 13. Effect of temperature and thus Damköhler number on uniformity of film growth in rectangular and V-shaped grooves at a constant pressure of 1 atm.

(g), (h) $Da = 50$.

portant in determining whether conclusions will be formed. At high temperature ($T = 1{,}616$ K) occlusions form for both large V-grooves, but step coverage in the small groove is still good. This phenomenon has also been observed experimentally in the deposition of *silicon* by CVD (Van den Brekel, 1977). The numerical simulation can thus be used to predict whether occlusions will form or finger formation will take place for specific deposition conditions and with a specific initial shape of groove. Note, however, that the present continuum model is valid only for cases where the MFP is shorter than the typical size of surface features, which is the case for pressures close to atmospheric ($0.1 \leq P \leq 1.0$).

Summary and Conclusions

In this article, a continuum model for interface evolution during typical atmospheric pressure CVD is presented. The effects of gas diffusion through a boundary layer, adsorption and desorption, capillarity, surface reactions, and solid phase surface diffusion are accounted for. A basic solution of the model is planar film growth, and a linear stability analysis is used to determine under which conditions this basic solution will become unstable. When this is the case, the model equations have to be integrated in time to determine the dynamic behavior of the interface and the morphology of deposition. The coupling between governing equations makes it worthwhile to attempt simplified solutions that are applicable in limiting cases. Two such simplified cases, namely, growth under diffusion-limited conditions ($Da \gg 1$) and growth under kinetic control ($Da \ll 1$), were considered. In both cases a much simpler system of equations was obtained and similarities and differences between these and the complete model were discussed.

The second part of the article focuses on solution of the complete system of equations. This enables us to follow the evolution of the gas–solid interface from any initial interface shape and for a wide range of deposition conditions. Important aspects of the solution method include the parametrization necessary to avoid problems with infinite gradients, and the automatic generation of an adaptive mesh at each point. Several numerical examples were also considered. It was found that the model correctly predicts experimentally observed phenomena, including the following: the decrease in film morphology with increase in temperature, the formation of deep grooves and fingers during diffusion-limited growth, the formation of semicircular structure where some caps (nodules) grow at the expense of others leading to the typical *growth–death* phenomenon, and the development of occlusions. The shape of isoconcentration lines in the gas phase was found to depend on the temperature and thus the Damköhler number. At high temperature ($\sim 1{,}600$ K) under diffusional control, they are close together above protrusions and rarefied in grooves and depressions, which explains preferential growth of fingers and the formation of grooves. At low temperature ($\sim 1{,}100$ K) under kinetic control, this is reversed. It was also found that a decrease in reactor pressure increases the uniformity of deposition and prevents finger formation.

The results indicate that the morphology of deposition is strongly dependent on the controlling mechanism of deposition, as characterized by the Damköhler number, Da. At low temperature and pressure (in our case 1,100 K and 0.1 atm), the process is limited by kinetics of surface reactions, in which case $Da \ll 1$ and film deposition is found to be very uniform. As the temperature and/or pressure is increased, diffusional limitations develop and preferential growth of protrusions take place, leading to a very nonuniform fingerlike structure at large Damköhler numbers ($Da \gg 1$). If a high temperature ($\sim 1{,}600$ K) has to be maintained to get a desired deposition rate, film uniformity can be improved by decreasing reactor pressure, which reduces diffusional limitations. Numerical results therefore suggest that to maintain uniform film growth, deposition conditions should be chosen in such a way that the lowest value of Da, the Damköhler number, is achieved.

Acknowledgments

The work was partially supported by the National Center for Supercomputing Applications under grant TRA940054N through the use of the CRAY Y-MP4/464 at NCSA, University of Illinois at Urbana-Champaign. Helpful discussions with Dr. J. M. Nitsche and Dr. D. Orlicki on the numerical solution procedure, and the mesh generation code of Dr. J. Degreve are greatly appreciated.

Notation

C = concentration, mol/m^3 or mol/m^2
C^* = function of ζ, used in linear stability analysis
$\mathcal{C}$ = dimensionless concentration, subscripts: 0—basic, 1—perturbed
D_{fs} = surface mobility, m^2/s
E_a = activation energy, J/mol
H^* = constant, used in linear stability analysis
k = reaction rate constant, mol/m$^2\cdot$s
k_1 = reaction rate constant, 1/s
k_{ad} = adsorption rate constant, m^3/mol
k_{des} = desorption rate constant, 1/s
K_{AD} = adsorption/desorption equilibrium constant, (mol/m^3)$^{-1}$
K_B = Boltzmann's constant, J/K
K_0 = preexponential factor, m/s
$K_1,\ldots,K_7$ = constants used in calculation of K, D_f, D_s^* and Γ
l = period of interface considered, m
$\boldsymbol{n}$ = vector normal to surface
N_{AV} = Avogadro's number
$R(C)$ = reaction term, mol/m$^2\cdot$s
t = time, s
T = substrate temperature, K
V = volume, m^3
z = vertical coordinate, m

Greek letters

β = molar volume, ΩN_{AV}, m^3/mol
γ = surface tension, J/m^2
η = L/δ
ξ = horizontal coordinate, dimensionless
τ = dimensionless time, tV_0/L
Ω = molecular volume, m^3

Literature Cited

Ananth, R., and W. N. Gill, "Criteria for Making Uniform Films by Chemical Vapor Deposition," *J. Cryst. Growth*, **118**, 60 (1992).
Bales, G. S., and A. Zangwill, "Macroscopic Model for Columnar Growth of Amorphous Films by Sputter Deposition," *J. Vac. Sci. Technol. A*, **9**(1), 145 (1991).
Bhatia, Q. S., and V. Hlavacek, "Integration of Difficult Initial and Boundary Value Problems by Arc-Length Strategy," *Chem. Eng. Commun.*, **22**, 287 (1983).
Bird, R. B., W. E. Stewart, and E. N. Lightfoot, *Transport Phenomena*, Wiley, New York (1960).
Brackbill, J. U., and J. S. Saltzmann, "Adaptive Zoning for Singular Problems in Two Dimensions," *J. Comp. Phys.*, **46**, 342 (1982).
Cale, T. S., and G. B. Raupp, "A Unified Line-of-Sight Model of Deposition in Rectangular Trenches," *J. Vac. Sci. Technol. B*, **8**(6), 1242 (1990).
Carberry, J. J., *Chemical and Catalytic Reaction Engineering*, McGraw-Hill, New York (1976).
Degreve, J., *Use of Adaptive Meshes in Simulation of Combustion Phenomena*, PhD Diss., SUNY at Buffalo, NY (1990).
Degreve, J., et al., "Use of 2-D Adaptive Mesh in Simulation of Combustion Front Phenomena," *Comput. Chem. Eng.*, **11**(6), 749 (1987).
Ettouney, H. M., and R. A. Brown, "Finite-Element Methods for Steady Solidification Problems," *J. Comp. Phys.*, **49**, 118 (1983).
Froment, G. F., and K. B. Bischoff, *Chemical Reactor Analysis and Design*, 2nd ed., Wiley, New York (1990).
Hoffmann, K. H., and J. Sprekels, eds., *Free Boundary Problems: Theory and Applications*, Vol. I, Wiley, New York (1990).
Kingery, W. D., H. K. Bowen, and D. R. Uhlmann, *Introduction to Ceramics*, 2nd ed., Wiley, New York (1976).
Kristyan, S., and J. A. Olson, "Statistical Mechanical Treatment of the Surface Free Enthalpy Excess of Solid Chemical Elements: 1. Temperature Dependence," *J. Phys. Chem.*, **95**, 921 (1991).
Kubicek, M., "Algorithm 502: Dependence of Solution of Nonlinear Systems on a Parameter," *ACM Trans. Math. Softw.*, **2**(1), 98 (1976).
Levenspiel, O., *Chemical Reaction Engineering*, 2nd ed., Wiley, New York (1972).
Mazor, A., D. J. Srolovitz, P. S. Hagen, and B. G. Bukiet, "Columnar Growth in Thin Films," *Phys. Rev. Lett.*, **60**(5), 424 (1988).
Messier, R., "Toward Quantification of Thin Film Morphology," *J. Vac. Sci. Technol. A*, **4**(3), 490 (1986).
Messier, R., and J. E. Yehoda, "Geometry of Thin Film Morphology," *J. Appl. Phys.*, **58**(10), 3739 (1985).
Movchan, B. A., and A. V. Demchishin, "Study of the Structure and Properties of Thick Vacuum Condensates of Nickel, Titanium, Tungsten, Aluminium Oxide and Zirconium Dioxide," *Fiz. Metal. Metalloved.*, **28**(4), 653 (1969).
Mullins, W. W., "Theory of Thermal Grooving," *J. Appl. Phys.*, **28**(3), 333 (1957).
Mullins, W. W., "Flattening of a Nearly Plane Solid Surface Due to Capillarity," *J. Appl. Phys.*, **30**(1), 77 (1959).
Oh, H. J., S. W. Rhee, and I. S. Kang, "Simulation of CVD Process by Boundary Integral Technique," *J. Electrochem. Soc.*, **139**(6), 1714 (1992).
Palmer, B. J., and R. G. Gordon, "Local Equilibrium Model of Morphological Instabilities in Chemical Vapor Deposition," *Thin Solid Films*, **158**, 313 (1988).
Palmer, B. J., and R. G. Gordon, "Kinetic Model of Morphological Instabilities in Chemical Vapor Deposition," *Thin Solid Films*, **177**, 141 (1989).
Paretta, A., G. Giunta, E. Capelli, V. Adoncecchi, and V. Vittori, "Influence of Substrate and Process Parameters on the Properties of CVD-SiC," *Mat. Res. Soc. Symp. Proc.*, **168**, 227 (1990).
Pelce, P., ed., *Dynamics of Curved Fronts*, Academic Press, Boston (1988).
Schmidt, W. U., *The Development of Chromium Diboride Fibers by CVD for Use as Reinforcement Material in Metal Matrix Composites*, PhD Thesis, SUNY at Buffalo, NY (1991).
Seydel, R., and V. Hlavacek, "Role of Continuation in Engineering Analysis," *Chem. Eng. Sci.*, **42**(6), 1281 (1987).
Singh, V. K., and E. S. G. Shaqfeh, "Effect of Surface Re-emission on the Surface Roughness of Film Growth in Low Pressure Chemical Vapor Deposition," *J. Vac. Sci. Technol. A*, **11**(3), 557 (1993).
Srolovitz, D. J., A. Mazor, and B. G. Bukiet, "Analytical and Numerical Modeling of Columnar Evolution in Thin Films," *J. Vac. Sci. Technol. A*, **6**(4), 2371 (1988).
Tait, R. N., T. Smy, and M. J. Brett, "Simulation and Measurement of Density Variation in Mo Films Sputter Deposited over Oxide Steps," *J. Vac. Sci. Technol. A*, **8**(3), 1593 (1990).
Thiart, J. J., V. Hlavacek, and H. J. Viljoen, "Simulation of the Growth of CVD Films," *Chem. Eng. Sci.*, in press (1995).
Thompson, J. F., Z. U. A. Warsi, and C. Wayne Mastin, *Numerical Grid Generation: Foundations and Applications*, Elsevier, New York (1985).
Thornton, J. A., "Influence of Apparatus Geometry and Deposition Conditions on the Structure and Topography of Thick Sputtered Coatings," *J. Vac. Sci. Technol.*, **11**(4), 666 (1974).
Van den Brekel, C. H. J., "Characterization of Chemical Vapour-Deposition Processes: I and II," *Philips Res. Rep.*, **32**, 118 (1977).
Van den Brekel, C. H. J., and A. K. Jansen, "Morphological Stability Analysis in Chemical Vapour Deposition Processes: I," *J. Crystal Growth*, **43**, 364 (1978a).
Van den Brekel, C. H. J., and A. K. Jansen, "Morphological Stability Analysis in Chemical Vapour Deposition Processes: II," *J. Crystal Growth*, **43**, 371 (1978b).
Viljoen, H. J., J. J. Thiart, and V. Hlavacek, "Controlling the Morphology of CVD Films," *AIChE J.*, **40**(6), 1032 (1994).

Manuscript received Aug. 22, 1994, and revision received Nov. 15, 1994.